ON A PHASE–BUNCHING MODEL FOR JOVIAN S–BURSTS

A. J. Willes*

Abstract

Motivated by recent observations of phase coherence in Jovian S–bursts, this paper re–examines a continuous feedback model in which phase–coherent radiation is generated by phase–bunched electrons in an interaction region within the Io flux tube. Evaluation of S–burst drift rates reveals that one of the unexplained properties of S–bursts, their complex morphologies, is a natural feature of a phase–bunching model.

1 Introduction

Electron Cyclotron Maser Emission (ECME) naturally accounts for many features of Jovian S–bursts, including the observed high brightness temperatures, narrow bandwidths, and beaming onto the surface of a hollow cone [Hewitt et al., 1981]. The upper cutoff frequency and the polarization sense of Jovian decametric radiation are consistent with extraordinary (x) mode emission at the electron cyclotron frequency Ω_e. In the Ellis model [Ellis, 1974], electrons are accelerated along the Io flux tube ($L = 5.9$) by the magnetic field–aligned potential induced by the motion of Io through the Jovian magnetosphere. The electrons propagate adiabatically, and are magnetically reflected in the converging field lines near the poles. The reflected electron distribution is unstable to wave growth via ECME, generating waves near Ω_e. The negative S–burst drift is attributed to the falling emission frequency as electrons propagate to higher altitudes where Ω_e is smaller. Reasonable agreement has been obtained between the Ellis model and observations; in particular, the prediction that the drift rate increases with increasing frequency before turning over at high frequencies close to the mirror point has been verified observationally [Zarka et al., 1996].

Despite the successes of the standard theory, significant discrepancies between observations and theory remain unresolved. For instance, the Ellis model predicts simple S–burst morphologies, with a constant drift rate. However, simple S–bursts are relatively uncommon; for instance, in one sample of nearly 1000 S–bursts, only 18% are simple S–bursts

*School of Physics, University of Sydney, NSW 2006, Australia

[Boudjada et al., 1995b]. The majority are complex S–bursts, with a variety of morphologies, including negative and positive drift rates within the same burst, and others where multiple branches diverge from a common burst segment [see Riihimaa, 1991, Figure 2, for a classification into specific types]. Microsecond–resolution observations reveal that the deceptively simple S–burst structure is in fact composed of many distinct sub–pulses, each lasting $40 - 200\,\mu$s, and the instantaneous wave frequency exhibits phase coherence over part or all of an individual sub–pulse [Carr and Reyes, 1999]. This is strongly indicative of a phase–coherent process, rather than ECME, for which wave growth is independent of phase.

The aim in this paper is to demonstrate that complex S–burst morphologies are consistent with a phase–bunching mechanism, which generates phase–coherent radiation. In Section 2, the main features of the original phase–bunching model for terrestrial VLF emissions are summarized. The application of this model to Jovian S–bursts is discussed in Section 3, together with an explanation for complex S–burst morphologies assuming a simplified Jovian dipole magnetic field model.

2 Phase–bunching model for terrestrial VLF emissions

Terrestrial VLF emissions are predominantly artificially generated (from whistlers, VLF transmitters and power line radiation), but also occur naturally in the outer magnetosphere [see review by Matsumoto, 1979]. A characteristic property of these emissions is that there is no threshold triggering wave amplitude, but there is a threshold trigger time, referred to as the dash–dot anomaly; dashes (150 ms) trigger emissions whereas dots (50 ms) do not. Phase–bunching occurs when electrons move towards a common gyration phase, either by being shifted axially (in the magnetic field direction) or azimuthally. In the Helliwell [1967] model, streaming electrons and whistler waves resonate within an Interaction Region (IR) which itself can drift along the magnetic field lines. Near resonance, energy is transferred from phase–bunched electrons to phase–coherent waves (or vice–versa). Electrons entering (say) the left–hand side of the IR are phase–bunched by oppositely–directed waves leaving the IR; the departing waves themselves having been generated earlier by a different bunch of electrons leaving the IR on the right–hand side. Thus electron bunching tends to occur on one side of the IR and wave growth on the other. The self–sustaining feedback process requires that the electrons and waves propagate in opposite directions in the IR rest frame. This constrains the IR drift velocity along the field lines to be in the range $v_{g\|} < v_{IR} < v_{\|}$ (for $v_{\|} > 0$ and $v_{g\|} < 0$).

Drift rates are derived in the Helliwell model by appealing to the *consistent wave condition*, which is that the wave–particle resonance condition

$$\Delta(s,t) = \omega(s,t) - \frac{\Omega_e(s)}{\gamma} - k_{\|}[\omega(s,t), \Omega_e(s)]\, v_{\|}(s,t) = 0\,, \tag{1}$$

is satisfied, together with the condition

$$d\Delta(s,t) = 0\,, \tag{2}$$

which ensures that the time of the resonant interaction is maximized by selecting only those electrons and waves that do not move out of resonance due to the field inhomogeneity. The parallel wavenumber $k_{\|}$ is determined by the wave dispersion relation, and the parallel electron velocity $v_{\|}$ and wave frequency ω are functions of both position s and time t, so that waves can resonate with different velocity components of the beam at different times.

The Helliwell model successfully explains many features of discrete VLF emissions, including variable drift rates and the triggering time (the delay in setting up the feedback process). However, there is no consensus in the literature regarding the specific wave amplification mechanism [Matsumoto, 1979]. It is likely, however, that mechanisms involving electrons phase–trapped by the whistler wave can be ruled out on the basis of the physical requirement that the trapping time be less then the electron propagation time across the IR. The implication that there is a minimum triggering wave amplitude is inconsistent with VLF triggering from low–power transmitters, which suggest that no such threshold amplitude exists [Winglee, 1985; Melrose, 1986b]. To avoid this problem, Winglee [1985] proposed a transitory wave growth mechanism involving untrapped, phase–bunched electrons. Identification of the wave amplification mechanism is not crucial to the S–burst drift rate analysis in the next Section, and will be deferred to future research.

3 Jovian S–burst drift rates

A modified phase–bunching model has previously been proposed for S–bursts [Ratner, 1976; Melrose, 1986a], based on the many similarities between terrestrial VLF emissions and S–bursts. Common characteristics include burst morphology, where both emissions have narrow bandwidths and positive and negative frequency drifts (sometimes within the same burst), phase coherence, and evidence for wave–electron–wave interactions in intersecting terrestrial VLF emissions [Helliwell, 1974] and S–burst interactions with narrowband, constant–frequency L–bursts [Ellis, 1974].

Significant modifications are necessary in applying the phase–bunching model to Jovian S–bursts. Most importantly, whistler waves are replaced by magnetoionic x–mode waves, with the consequence that the requirement that the parallel whistler wave group velocity and electron velocity must be in opposite directions, is reversed so that the parallel x–mode wave group velocity and electron velocity must be in the same direction. The constraint that v_{IR} lies somewhere in between then requires that $|v_{IR}| > 0$, i.e., the IR must drift (whereas in the terrestrial case, the IR can be at rest). Another difference is that phase bunching is axial for parallel–propagating whistler waves, and is a nonrelativistic phenomenon [e.g., Lutomirski and Sudan, 1964], whereas for parallel–propagating x–mode waves, the azimuthal bunching is an intrinsically relativistic effect [Sprangle and Manheimer, 1975]. However, this has little bearing on predictions of S–burst drift rates.

In order to discuss S–burst drift rates, assuming a phase–bunching mechanism, we adopt a simplified model with the following assumptions: (a) Jupiter's magnetic field is dipolar, with a dipole moment of 10 G R_J^3, which is a reasonable approximation to field strengths in the decametric emission region [Krausche et al., 1976]. (b) Streaming electrons propagate

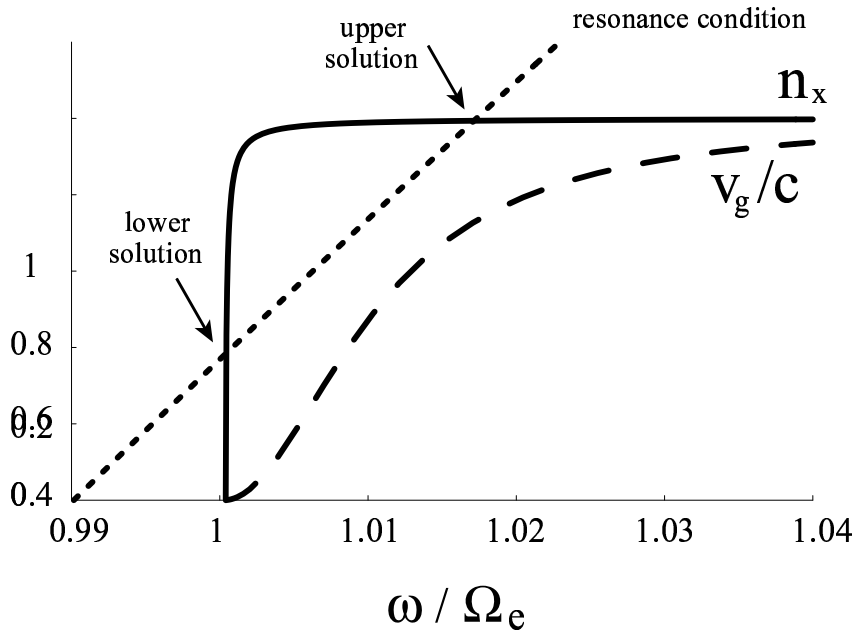

Figure 1: The intersection of the resonance condition (dotted curve), expressed in the form $n(\omega/\Omega_e)$, with the x–mode dispersion relation (solid curve) generally yields an "upper" and "lower" solution.

adiabatically in the Io flux tube, with parameters $v_{\rm beam}/c = 0.14$, $\Delta v_{\rm beam}/v_{\rm beam} = 0.2$, and equatorial pitch angle = 0.05 rad. (c) Constant plasma density in the source region, with $\omega_p/\Omega_e = 0.02$. (d) This model does not prescribe the value or variation in v_{IR}, except for the constraint that the waves and electrons propagate in opposite directions in the IR rest frame, with

$$\min[|v_{g\parallel}|, |v_\parallel|] < |v_{IR}| < \max[|v_{g\parallel}|, |v_\parallel|]\,. \tag{3}$$

As discussed by Helliwell [1967], the IR will drift so as to maintain a balance, in the IR rest frame, between the output wave power and the input power transferred from phase–bunched electrons. A more sophisticated model incorporating wave–particle interactions is necessary to adequately model the IR drift.

The S–burst drift rate is derived from equation (2), yielding the expression:

$$\frac{d\omega}{dt} = \frac{v_\parallel \left[\left(\frac{1}{\gamma} + v_\parallel \frac{\partial k_\parallel}{\partial \Omega_e}\right)\frac{\partial \Omega_e}{\partial s} + k_\parallel \frac{\partial v_\parallel}{\partial s}\right]}{\left(1 - \frac{v_\parallel}{v_{g\parallel}}\right)\left(1 - \frac{v_\parallel - v_{IR}}{v_{g\parallel} - v_{IR}}\right)}\,. \tag{4}$$

There are typically two solutions when the resonance condition (1) is solved with the x–mode dispersion relation, as shown in Figure 1. The "lower" solution occurs near the x–mode cutoff frequency and corresponds to x–mode waves with very low group speeds. The "upper" solution has $n \approx 1$ and group speeds comparable to c.

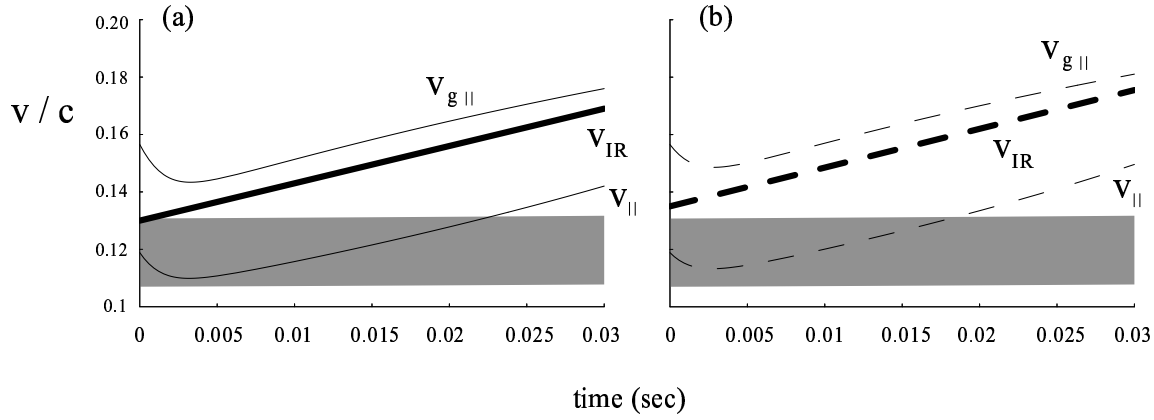

Figure 2: Evolution of resonant parallel electron ($v_\parallel$) and wave ($v_{g\parallel}$) velocities during an S–burst. The shaded region corresponds to the available range of electron beam speeds at the IR position; (a) initial $v_{IR} = 0.13\ c$, (b) initial $v_{IR} = 0.135\ c$.

For "upper" x–mode waves with $n \approx 1$ and $|v_{g\parallel}| \gg |v_\parallel|$, equation (4) simplifies to

$$\frac{d\omega}{dt} \approx \frac{v_\parallel}{\gamma}\,\frac{\partial \Omega_e}{\partial s} \tag{5}$$

which is the drift rate predicted by the Ellis model. Figure 2 shows how the resonant velocities $v_\parallel$ and $v_{g\parallel}$ vary during an S–burst, by solving the differential equation (4) with (1) and the initial condition that the waves are initially in resonance with the mid–beam velocity, assuming an initial IR position (measured on the $L = 5.9$ field line from the Jovian surface in the northern hemisphere) $s = 0.5\,R_J$, and emission propagation angle (relative to $\mathbf{B}$) $\chi = 1.35$ rad. In this particular example, v_{IR} is assumed to increase linearly throughout the life of the S–burst. The S–burst cuts out when the resonant electron speed $v_\parallel$ exceeds the range of available electron beam speeds at the IR position (shaded region in Figure 2). This occurs at time $t = 0.023\,\mathrm{s}$ in Figure 2a and at time $t = 0.018\,\mathrm{s}$ in Figure 2b (with a higher initial v_{IR}). The S–burst frequency–time profile for the S–bursts in Figure 2 is displayed in Figure 3a. The x–mode wave group speed is a sensitive function of the ratio ω/Ω_e (see Figure 1), so that the variation in ω/Ω_e over the life of the S–burst (evident in Figure 3c) corresponds to a significant variation in group speeds ($\approx 15\%$ in Figure 3d). One consequence of this is that there are significant dispersion delay effects as the S–burst propagates out through the Jovian magnetosphere, which distorts the S–burst profile, as shown in Figure 3b. As the waves propagate into decreasing magnetic field strengths, Ω_e decreases, so that the ratio ω/Ω_e increases. The waves thus effectively move to the right on the dispersion curve in Figure 1 and consequently the group speed approaches c. The propagation time to a remote observer as a function of S–burst frequency is $T(\omega) = \int dl\,[v_g(\omega, l)]^{-1}$, where l is the distance along the radiation path. S–burst frequencies with relatively low initial group speeds are thus delayed with respect to the remainder of the S–burst, leading to a distortion of the S–burst profile. The profile in Figure 3b is evaluated for the downward–propagating ray in the plane of the Io–flux tube, assuming that the ray is unrefracted. This assumption is sufficient to demonstrate the

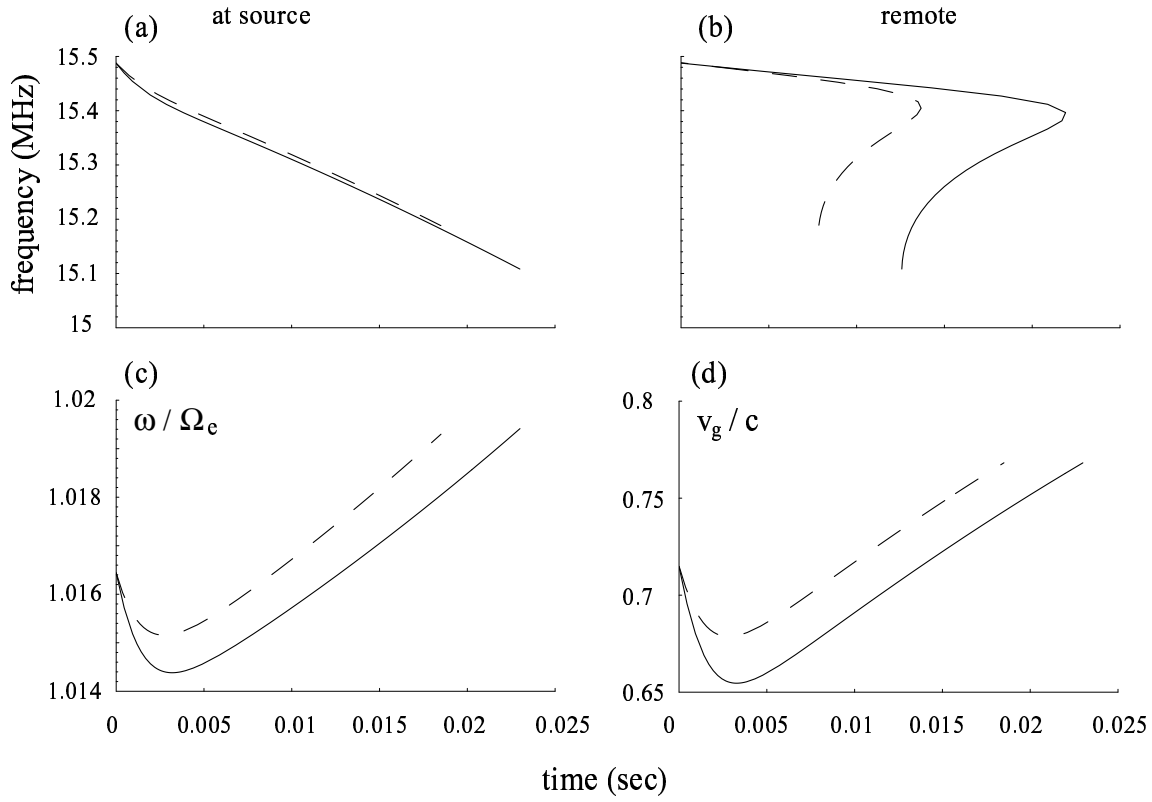

Figure 3: (a) S–burst frequency–time profile, where the solid curve corresponds to the S–burst in Figure 2a and the dashed curve to Figure 2b; (b) the same profile after the S–burst has propagated through the Jovian magnetosphere; (c) the ratio of wave frequency ω to the local electron cyclotron frequency Ω_e at the IR position; and (d) the group speed.

importance of dispersion delay effects; however, a more accurate model would incorporate geometric ray tracing and a more realistic electron–density model. The S–burst profile in Figure 3b, with apparently converging negative and positive drift branches, is comparable to type f S–bursts in the Riihimaa [1991] classification. Slight variations in v_{IR} can significantly alter S–burst morphologies; for example, two simultaneous IRs in the source region with slightly different initial drift speeds (the solid and dashed curves in Figure 3b) produce two diverging branches from a common stem [c.f. Riihimaa, 1991, types i, j, k]. If v_{IR} decreases with time during the S–burst, the group speed also tends to decrease, leading to decreasing S–burst drift rates with time [c.f. Riihimaa, 1991, types b, c, d].

It is important to point out that the complex S–burst profiles predicted by the phase–bunching model cannot be produced in the standard Ellis/ECME model, because ω/Ω_e, and hence v_g, remain constant throughout the S–burst, and the constant–drift S–burst profile remains undistorted as the S–burst propagates through the Jovian magnetosphere to a remote observer.

The "lower" S–burst drift rates differ markedly from the Ellis prediction (5), as shown in Figure 4. The S–burst frequency is nearly constant (marginally positive drift rate)

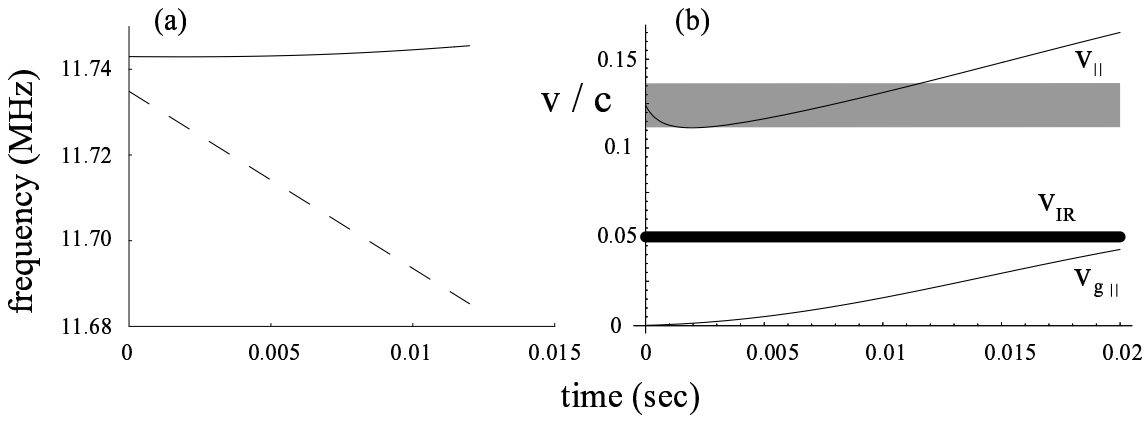

Figure 4: S–burst characteristics for the "lower" x–mode solution, with parameters $s_{\rm initial} = 0.65\,R_J$, $\chi = 1.46$ *rad, and* $v_{IR} = 0.05\,c$. *The solid curve is the (undistorted) S–burst frequency–time profile, and the dashed curve is the local* Ω_e *at the IR position [corresponding to the Ellis model drift rate (5)].*

in comparison with the negative Ellis drift rate (dashed line). The possible relation to constant–frequency, narrowband emissions [e.g., Ellis, 1974] will be explored in future work.

Other important considerations which warrant further investigation include an assessment of the suitability of assuming cold plasma magnetoionic x–mode dispersion, given the strong dependence of x–mode dispersion near the cutoff frequency to the relative hot and cold electron densities [Le Queau and Louarn, 1989]. By way of comparison, the source region for terrestrial AKR consists almost entirely of hot electrons, due to the removal of background plasma by magnetic–field aligned electric fields [Ergun et al., 2000]. The significant influence of parallel electric fields on S–burst drift rates also needs to be taken into account [Melrose, 1986a].

References

Boudjada, M. Y., H. O. Rucker, H. P. Ladreiter, and B. P. Ryabov, Jovian S–bursts: the event of 4 January 1993, *Astron. Astrophys.*, **295**, 782, 1995b.

Carr, T. D., and F. Reyes, Microstructure of Jovian decametric S–bursts, *J. Geophys. Res.*, **104**, 25, 25127–25142, 1999.

Carr, T. D., and F. Reyes, Microstructure of Jovian decametric S–bursts, *J. Geophys. Res.*, **104**, 25127, 1999.

Ellis, G. R. A., The Jupiter radio bursts, *Proc. Astron. Soc. Aust.*, **2**, 236–243, 1974.

Ergun, R. E., C. W. Carlson, J. P. McFadden, G. T. Delory, R. J. Strangeway, and P. L. Pritchett, Electron–cyclotron maser emission driven by charged–particle acceleration from magnetic field–aligned electric fields, *Astrophys. J.*, **538**, 456, 2000.

Helliwell, R. A., A theory of discrete VLF emissions from the magnetosphere, *J. Geophys. Res*, **72**, 4773, 1967.

Helliwell, R. A., Controlled VLF wave injection experiments in the magnetosphere, *Space Sci. Rev.*, **15**, 781, 1974.

Hewitt, R. G., D. B. Melrose, and K. G. Rönnmark, A cyclotron theory for the beaming pattern of Jupiter's decametric radio emission, *Proc. Astron. Soc. Aust.*, **4**, 221, 1981.

Krausche, D. S., R. S. Flagg, G. R. Lebo, and A. G. Smith, High resolution spectral analyses of the Jovian decametric radiation. I. Burst morphology and drift rates, *Icarus*, **29**, 463, 1976.

Le Queau, D., and P. Louarn, Analytical study of the relativistic dispersion: Application to the generation of the auroral kilometric radiation, *J. Geophys. Res.*, **94**, 2605, 1989.

Lutomirski, R. F., and R. N. Sudan, Exact nonlinear electromagnetic whistler modes, *Phys. Rev.*, **147**, 156, 1964.

Matsumoto, H., Nonlinear whistler–mode interaction and triggered emissions in the magnetosphere: A review, in *Wave Instabilities in Space Plasmas*, edited by P. J. Palmadesso and K. Papadopoulos, 163, D. Reidel, Hingham, Mass., 1979.

Melrose, D. B., A phase–bunching mechanism for fine structures in auroral kilometric radiation and Jovian decametric radiation, *J. Geophys. Res.*, **91**, 7970, 1986a.

Melrose, D. B., Instabilities in Space and Laboratory Plasmas, Cambridge University Press, p. 241, 1986b.

Ratner, M. J., On the possibility of nonlinear phase bunching effects in the extraordinary mode decametric radio emission of Jupiter, *Astroph. J.*, **209**, 945, 1976.

Riihimaa, J. J., Evolution of the spectral fine structure of Jupiter's decametric S–storms, *Earth, Moon and Planets*, **53**,157, 1991.

Sprangle, P., and W. M. Manheimer, Coherent nonlinear theory of a cyclotron instability, *Phys. Fluids*, **18**, 224, 1975.

Winglee, R. M., Enhanced growth of whistlers due to bunching of untrapped electrons, *J. Geophys. Res.*, **90**, 5141, 1985.

Zarka, P., T. Farges, B. P. Ryabov, M. Abada–Simon, and L. Denis, A scenario for Jovian S–bursts, *Geophys. Res. Lett.*, **23**, 125, 1996.